

Surface Modification of Silica Fume with Amine Groups to Reduce Agglomeration and Improve Asphalt Resistance to Oxidation

Nader Abutalib^{1*}, Sidharth Reddy Karnati², Daniel Oldham², Lifeng Zhang² and Elham Fini³

¹Department of Computational Science and Engineering, North Carolina A&T State University, Greensboro, North Carolina, USA

²Department of Nanoengineering, Joint School of Nanoscience and Nanoengineering, North Carolina A&T State University, Greensboro, North Carolina, USA

³Department of Civil and Environmental Engineering, North Carolina A&T State University, Greensboro, North Carolina, USA

Research Article

Received: 26/12/2016

Accepted: 12/01/2017

Published: 20/01/2017

*For Correspondence

Nader Abutalib, Department of Computational Science and Engineering, North Carolina A&T State University, Greensboro, North Carolina, USA, Tel: 954-736-9351

Email: ntabutal@aggies.ncat.edu

Keywords: Silica fume modified binder (SFMB), Amine groups, Phosphonate, Asphalt oxidative aging, Agglomeration

ABSTRACT

This paper presents a rheological study of the design and development of surface-modification schemes for silica fume particles to improve their dispersion in asphalt and increase the asphalt aging resistance. The nanoparticle surface design involves an optimum balance of the use of inert and active surface functional groups to achieve minimal nanoparticle agglomeration and enhance the reduction in oxidative aging of silica-fume-modified asphalt binder. Silica fume particles with different functional groups, including amine and phosphonate groups, were produced. Agglomeration studies using SEM and zeta potential analysis indicate that modifying asphalt binder with amine-modified silica fume particles can reduce the agglomeration of the silica fume particles. The performance characteristics of functionalized silica fume particles and non-functionalized silica fume particles are compared with those of base asphalt. The following research hypotheses were investigated: silica fume will enhance asphalt's aging resistance; and amine groups will react with a high percentage of agglomerated silica fume particles in asphalt to reduce the agglomeration and increase the aging resistance. A rotational viscometer was used to study the effect of functionalized-silica-fume-modified binder on the high-temperature properties of the asphalt binder. Fourier transform infrared spectroscopy analysis was used to determine the chemical compounds of the amine-group silica-fume-modified binder matrix. Scanning electron microscopy was used to observe the surface morphology and analyze microstructure characteristics of materials. Using these surface-modification schemes, fluorescent silica fume particles can be more readily conjugated with asphalt molecules and used as highly fluorescent, sensitive, and reproducible labels in asphalt applications.

INTRODUCTION

The chemical and physicochemical mechanisms in asphalt oxidative aging have been the subject of extensive research for decades. A previous study used silica fume, an industrial waste, to decrease the rate of asphalt oxidation. The introduction of 4% silica fume to asphalt reduced asphalt oxidation aging; however, the main challenge with the use of high amounts of silica fume was found to be the agglomeration of nanoparticles to form micro-size clusters that reduce silica fume's effectiveness while making asphalt binder more susceptible to shear ^[1]. They then showed that a swine-manure-derived bio-binder, which has molecules of amine groups, has been used as a partial modifier to silica-fume-modified binder to improve the binder's rheological and mechanical properties while reducing the agglomeration. It significantly helped disperse the silica fume agglomeration and improve the aging resistance of the silica-fume-modified binder.

To find ways to introduce organic functional groups onto the surfaces of silica particles, a study controlled the surface expression of functional groups on silica particles. The study found that surface properties of silica materials are largely affected by the nature of the surface functional groups. It demonstrated that the degree of surface functionalization of the silica particles varied with the time of organosilane addition. For each type of amine-terminated organosilane used, the highest surface availability of organo-functional groups was obtained when the organosilane was added 30 min after particle growth was initialized. A progressive decrease in the surface availability of primary amine groups was observed when 3-aminopropyltrimethoxysilane (APTMS) was added later than 30 min after particle formation was initiated.

Amines are the groups which are used as antistripping agents for aggregates. Silica nanoparticles are coated with APTES which provides amines on the surface of silica. Amines on silica form a strong bond between bitumen and silica, which can withstand the action of water and significantly improve the adhesion [2]. Phosphorous acid (phosphate ester) is alternative stripping agent for asphalt and mineral aggregates [3]. THPMP chemical contains phosphate group, coating THPMP to silica helps to increase the zeta potential and being more anion in nature. By combining the APTES and THPMP increases the stability of the particle of silica nanoparticle [4].

Main aim of this paper is to form a chemical bond between silica fume and asphalt for better dispersion. It is an attempt to have amine group APTES on the surface and to stabilize particle using THPMP which can also be used as stripping agent for silica fume.

BACKGROUND

Silica nanoparticles are being used in many applications such as bioanalysis and biomedicine, ultra-high-throughput screening, chip-based technology, multi-target detection systems, and diagnostic screening. It has been shown that the high sensitivity provided by the fluorescence signal enhancement, selectivity, and reproducibility of nanoparticle-based bioassays can be inhibited by the tendency of the silica nanoparticles to aggregate, leading to reduced nanoparticle nonspecific binding. This tendency to aggregate is attributed to the large hydrodynamic size and large surface area of the silica nanoparticles. It has been hypothesized that to obtain successful and reproducible detection of biological targets using these fluorescent labels, the silica nanoparticles must be well dispersed in aqueous solution with minimal to no aggregation and nonspecific binding to biomolecules or substrates. Results indicated that adding to the surface of silica nanoparticles an appropriate ratio of inert functional groups (e.g., methyl phosphonate) to active functional amino groups results in a highly negative zeta potential, which is necessary to keep the particles well dispersed and at the same time enable amine-based bio-conjugation [4].

It has been documented that rutting susceptibility decreases asphalt mixtures' performance. A study aimed to improve the overall performance of asphalt binders and mixtures by modifying them with micromaterials and nanomaterials, including carbon microfiber, Nanomer nanoclay, nanosilica, unmodified nanoclay, and polymer-modified nanoclay. The microstructures of original materials and modified asphalt binders were observed using a field emission scanning electron microscope (FE-SEM). Performance tests were employed to evaluate the resistance to rutting and permanent deformation of the modified asphalt mixtures [5]. Test results indicated that the dynamic modulus of micromodified and nanomodified asphalt mixtures improved significantly; the rutting susceptibility of the modified asphalt mixtures was reduced significantly.

To improve asphalt's resistance to rutting and fatigue cracking, a study characterized the effect of nanosilica and diatomite modifiers on the physicochemical and rheological properties of binders at unaged and oxidized conditions, with the aim of predicting their field performance. Several rheological tests were developed using a dynamic shear rheometer, rutting resistance characterization, fatigue resistance characterization, and a surface free energy approach. Results indicated that modification of asphalt binder with chemically similar additives can result in materials with different physicochemical and mechanical responses. The physicochemical transformations taking place during aging influence the resulting performance of the aged binder. Modified asphalt showed less resistance to moisture damage [6].

It has been documented that agglomeration of nanoparticles negatively impacts the performance of carbon materials based on coal-tar pitch (CTP). Maciej et al. [7] hypothesized that the dispersion of CTP by selected nanoparticles as a binder precursor for the manufacture of synthetic carbon materials will impact on the structure of the resulting synthetic carbon materials with the de-agglomeration of nano-clusters. The objective of the research was to determine the optimal processing parameters of the dispersion of selected nanoparticles (graphene, carbon black, and nano-silicon carbide) in CTP and assess their impact on the structure of the resulting synthetic carbon materials. Nanoparticles were subjected to sonication. Various dispersants were used to prepare the suspensions: water, ethanol, dimethylformamide (DMF), and N-methylpyrrolidone (NMP). To sum up, DMF and NMP were found to be effective dispersants for the preparation of homogeneous nanoparticle-containing suspensions. The presence of SiC and carbon black nanoparticles in the liquid pitch during heat treatment up to 2000 °C leads to the inhibition of crystallite growth in carbon residue [7].

The formation of oxidation products changes the chemical composition of asphalt and leads to an increase in the overall stiffness and brittleness. A study was conducted using molecular dynamics simulation to investigate the oxidative aging effect of asphalt binder. The asphalt molecular models were validated in terms of thermodynamic properties such as density, surface

energy, viscosity, and cohesive energy density. The molecular structures of virgin and aged asphalt were analyzed by mean square displacement (MSD) and radial distribution function (RDF) of molecules and diffusion coefficient. Oxidative aging increased the density, viscosity, and cohesive energy density, but reduced surface free energy^[8]. The SARA fractions showed that oxidative aging weakens the nano- aggregation behavior of asphaltene molecules and reduces the translational mobility of asphalt molecules. Virgin asphalt has a lower activation energy barrier and thus has stronger instantaneous healing ability. The aged asphalt showed less resistance to moisture damage compared to virgin asphalt.

INVESTIGATED MATERIALS

Silica fume is an industrial waste material consisting of amorphous silica that is produced by electric arc furnaces as a byproduct of the production of elemental silicon or ferrosilicon alloys. The silica fume was acquired through Norchem Company, located in Hauppauge, NY. The silica fume has 100 nm – 600 nm average particle size. A SEM image indicates no agglomeration occurred when a small amount (0.1 mg) of silica fume was dispersed in water and sonicated at 500 W (**Figure 1a**). When the procedure was repeated with a larger amount (1 gm) of silica fume, the particles agglomerated because of the high surface energy (**Figure 1b**).

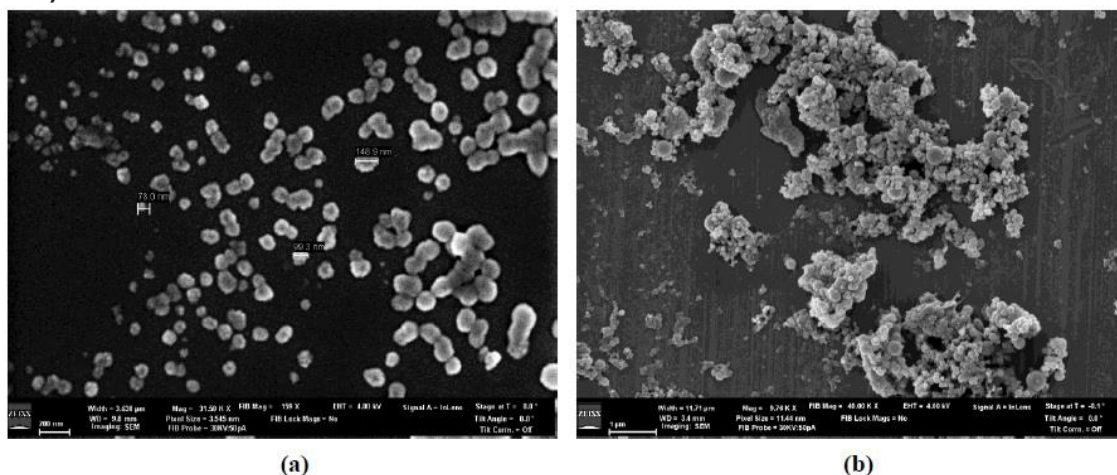


Figure 1. (a) 0.1 gm silica fume particles in water; (b) 1 gm silica fume particles in water.

Silica fume was used as an additive to asphalt binder to reduce oxidative aging. Binder modified with a 2% and 4% amount of silica fume showed significant aging resistance while 8% silica fume represents lower aging resistance^[4]. No agglomeration was occurred with the addition of low amount of silica fume up to 4% (**Figure 2a**). Modifying the binder with a higher percentage (8%) of silica fume showed particles agglomeration which indicated the decrease of aging resistance (**Figure 2b**). This decrease was linked to the degree of agglomeration in binder modified with a high concentration of silica fume. Agglomeration has been recognized as a problem in dealing with nanomaterials.

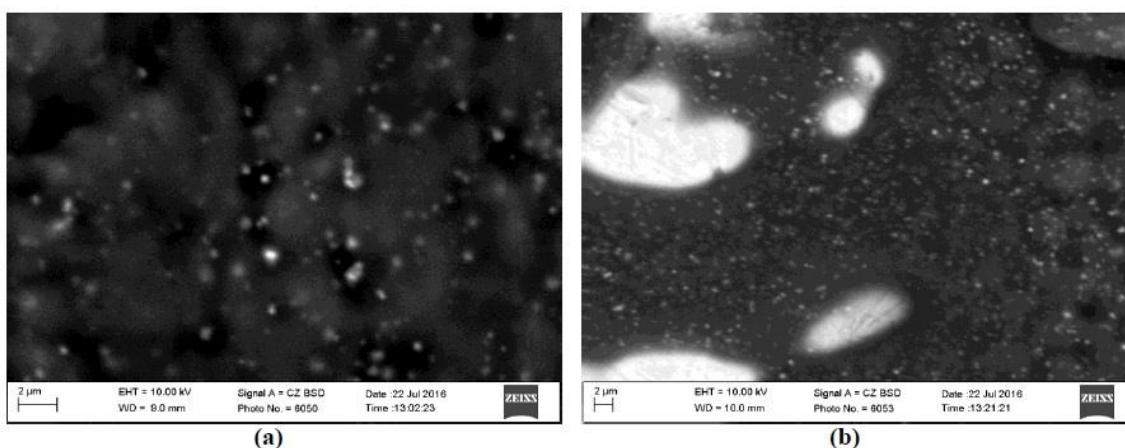


Figure 2. (a) SEM image of binder modified with 4% silica fume; (b) SEM image of binder modified with 8% silica fume.

To reduce the agglomeration of silica fume and improve oxidative aging performance, silica fume was functionalized with 5% bio-binder that has been converted from liquefied swine manure produced at our Sustainable Infrastructure Materials Laboratory. For binder modified with this functionalized silica fume, the VAI was significantly reduced, chemical characterization demonstrated a significant change in terms of carbonyl-dioxide, and SEM indicated dispersion of the agglomeration (**Figure 3**). Bio-binder which contains Amin group showed significant improvement in aging resistance. Therefore, APTES has been chosen in this paper as pure chemical of Amin group to functionalize the silica fume particles.

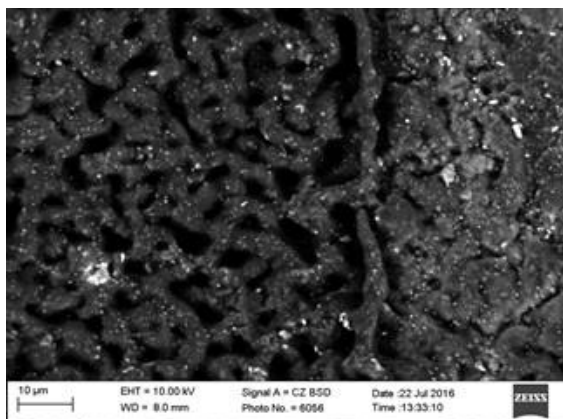


Figure 3. SEM image of binder modified with 8% silica fume that had been functionalized with 5% bio-binder.

OBJECTIVES

Research has shown that the introduction of silica fume to asphalt binder can reduce oxidative aging of the asphalt. While silica fume up to 4% (by weight of asphalt) was found to be very effective, no improvement was observed when 8% silica fume was used. This was attributed to the issue of agglomeration of silica fume nanoparticles, which occurs when a high amount of silica fume is used. Therefore, this paper aims to:

- Develop a simple preparation procedure for the introduction of different functional groups (including amine groups) into the silica fume surface.
- Minimize silica fume aggregation by introducing an optimum balance of inert and active functional groups.
- Explore the mechanism of silica fume agglomeration reduction induced by the addition of inert functional groups.

EXPERIMENT PLAN

Materials

The control binder used in this study is asphalt binder penetration grade PG 64-22 mixed with 8% industrial waste silica fume (SF). The silica fume surface was modified by adding aminopropyltrimethoxysilane (APTES) or 3-(Trihydroxysilyl) propylmethylphosphonate (THPMP). Then the modified silica fume was blended with asphalt binder for both aged and non-aged samples, and these modified binders were compared to 8% silica fume modified binder (SFMB). Short-term laboratory aging of the binders was performed using the rolling thin film oven (RTFO) and was executed in accordance with ASTM D2872^[9]. Following RTFO aging, PAV aging was performed following ASTM D6521^[10].

Fabrication of Silica Fume Surface Modification

Silica fume was functionalized by adding APTES or THPMP. Dynamic light scattering (DLS – Malvern Zetasizer nano range) was used to determine the hydrodynamic diameter (which is more than the actual diameter) and zeta potential. For this study, 0.5 gm of silica fume nanoparticles were used for surface modification with different APTES concentrations, following the procedure shown in Figure 4. The particle size and zeta potential were analyzed using 0.1 mg of silica fume dispersed in one liter of deionized water and sonicated for 5 min at 500 W, and from this mixture, a 1 ml sample was used for DLS measurement.

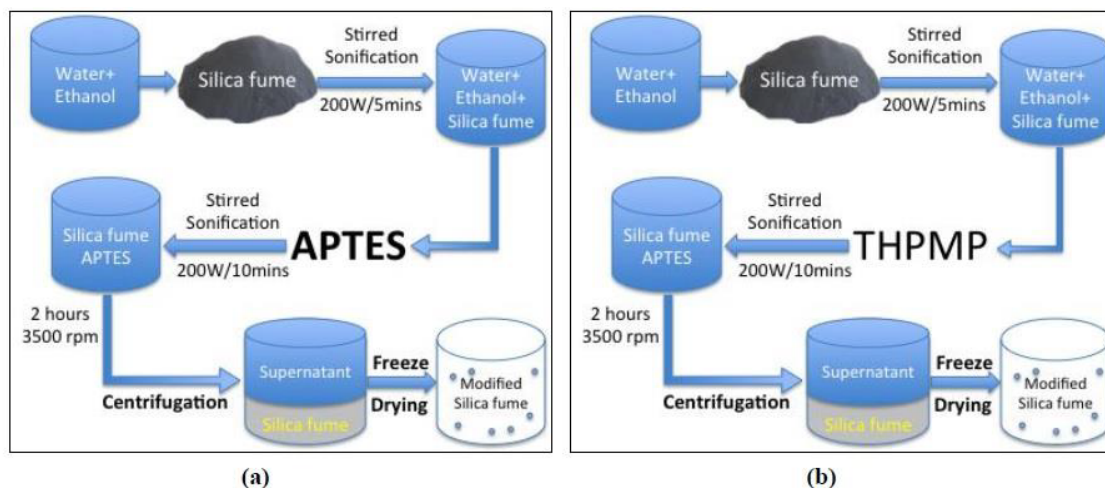


Figure 4. (a) APTES Surface Functionalization of Silica Fume; (b) THPMP Surface Functionalization of Silica Fume.

Rheological Characterization

Viscosity results were determined using a Brookfield rotational viscometer following ASTM D4402 [14]. Tests were conducted at 135 °C and 20 RPM. Samples were first preheated in the oven for 45 minutes then placed in the testing apparatus for 30 minutes to ensure the testing spindle, binder sample, and the testing apparatus were all in thermal equilibrium. In addition, the Malvern Kinexus dynamic shear rheometer (DSR) was utilized for investigating the viscoelastic properties, at intermediate temperature, of the samples according to ASTM D7175-15 [12,13]. The results were given in terms of complex shear modulus (G^*), which is described as a measure of the total resistance to deformation after exposure to repeated pulses of shear stress as shown in eqn (1). The DSR sweep test was run under strain-controlled modes at 31 frequencies ranging between 0.1 and 100 rad/s from 76 °C to 4 °C at 6-degree increments. For high intermediate temperatures, the 25 mm spindle was utilized while the 8 mm was used for low intermediate temperatures.

$$G^* = \frac{\tau_{max}}{\gamma_{max}} \tag{1}$$

Where

$$\gamma_{max} = \left(\frac{\theta r}{h} \right) \text{ and } \tau_{max} = \frac{2T}{\pi r^3}$$

where

τ_{max} : maximum applied stress

γ_{max} : maximum resultant strain

T: maximum applied torque

r: specimen radius

θ : deflection (rotation) angle (in radians)

h: specimen height

Fourier Transform Infrared Spectroscopy (FTIR)

Fourier transform infrared spectroscopy (FTIR) was used to determine various functional groups in asphalt modified with silica fume that occurred due to synthesis of the material. This test was conducted at room temperature for all samples using a Varian 670-IR with a diamond crystal. Before testing samples, the FTIR surface was cleaned using isopropanol and purged with a nitrogen flow of 25 psi. The number of scans was set to 300 with a resolution of 4 cm^{-1} with a scan range of 400 to 4000 cm^{-1} . To determine the variation in the chemical structure of binder before and aging, the areas of interest were that of the carbonyl ($I_{c=0}$) and the sulphoxide ($I_{s=0}$). A minimum of three replicates from three different sampling spots were performed to ensure that the final spectra best represents the entire sample. The areas under each peak were determined using Equations 2 and 3.

$$I_{c=0} = \frac{\text{Area of the carbonyl band around } 1,700 \text{ cm}^{-1}}{\text{Area of spectral bands between } 2,000 \text{ and } 600 \text{ cm}^{-1}} \tag{2}$$

$$VAI = \frac{\text{Aged viscosity value} - \text{Unaged viscosity value}}{\text{Unaged viscosity value}} \tag{3}$$

Scanning Electron Microscope (SEM)

A Carl Zeiss EVO LS 10 SEM was used for microstructure characterization and analysis of the SFMB specimens. The EVO LS 10 has full environmental capabilities to capture nano-scale interactions of samples under various temperatures, pressures, and humidity levels. It includes EVO HD, which further increases image resolution and contrast using a high-definition beam-source technology with low acceleration voltages. The experiments were conducted using VPSE (variable pressure secondary electron) and BSD (backscatter detector) at low vacuum (variable pressure) mode (0.5-0.6 mbar).

RESULTS AND DISCUSSION

Dynamic Light Scattering (DLS)

The plots in **Figure 5** are percentage of number of particles versus the diameter of particles. The plots show that the peaks are moving towards smaller diameter as the concentration of APTES increases from 0.3 gm to 0.8 gm and moving away as APTES concentration increases from 0.8 gm to 1.5 gm. The Polydispersity Index (PDI) was lowest for 0.8 gm APTES modified silica fume, with a PDI=0.35. (Moderate polydispersity is a PDI of 0.1 to 0.4, and broad polydispersity is a PDI greater than 0.4).

Zeta Potential (ZP)

Figure 6 represents the mean hydrodynamic diameter and zeta potential for concentrations of APTES on silica fume from 0.3 to 1.5 gm. The tests were conducted to optimize the amount of additional APTES to achieve the highest stability of the particles,

which implies smallest size. The size of APTES-modified SF particles at 0.3, 0.5, 0.8, 1.0, and 1.5 gm APTES concentration was 362.8, 379.4, 320.7, 472.0, and 505.3 nm, respectively. The best size of APTES-modified SF particles was obtained at an APTES concentration of 0.8 gm; above an 0.8 gm concentration of APTES, the size increased, which implies agglomeration of the particles, as shown by the PDI values given in **Figure 5**. **Figure 6** shows that the size distribution peaks of 0.5 and 0.8 gm APTES concentration were similar, but the average particle size is larger for 0.5 gm APTES concentration than for 0.8 gm APTES concentration, which is also indicated by the PDI values. Zeta potential values for APTES-modified SF particles at 0.3, 0.5, 0.8, 1.0 and 1.5 gm APTES concentration were -25.8, -27.2, -28.8, -17.7, and -10.5 mV. Zeta potential value directly addresses the size of the particles; the highest zeta potential number will indicate the lowest size. The highest zeta potential obtained was at 0.8 gm APTES concentration, while the lowest was at 1.5 gm APTES concentration. As the concentration of amines increased after the saturation point (0.8 gm), amines particles aggregated by backbonding to the surface silanol group. The zeta potentials of 0.5 and 0.8 gm APTES concentrations were similar. The best candidates were 0.5 and 0.8 gm APTES concentrations. Based on size, PDI, and zeta potential, the 0.8 gm APTES concentration was selected as better than the 0.5 gm APTES concentration. APTES-modified silica particles (-28.8 mV) have better zeta potential than the pristine silica fume particles (-27.3 mV), while the APTES-modified SF particles (320.7 nm) are bigger than the pristine silica fume particles (297.0 nm), with the advantage of having amine groups on the surface of the silica fumes. THPMP modified silica fume when mixed with asphalt we can see that the viscosity is not lower than that of APTES modified silica fume mixed with asphalt. Their zeta potential of THPMP on silica fume was -28 mV, when THPMP added to APTES modified silica fume particle the zeta potential has increased to -32 mV which shows better stability than APTES modified and THPMP modified alone [14-16]. The zeta potential of THPMP on silica fume was -28 mV, when THPMP added to APTES modified silica fume particle the zeta potential has increased to -32 mV which shows better stability than APTES modified and THPMP modified alone.

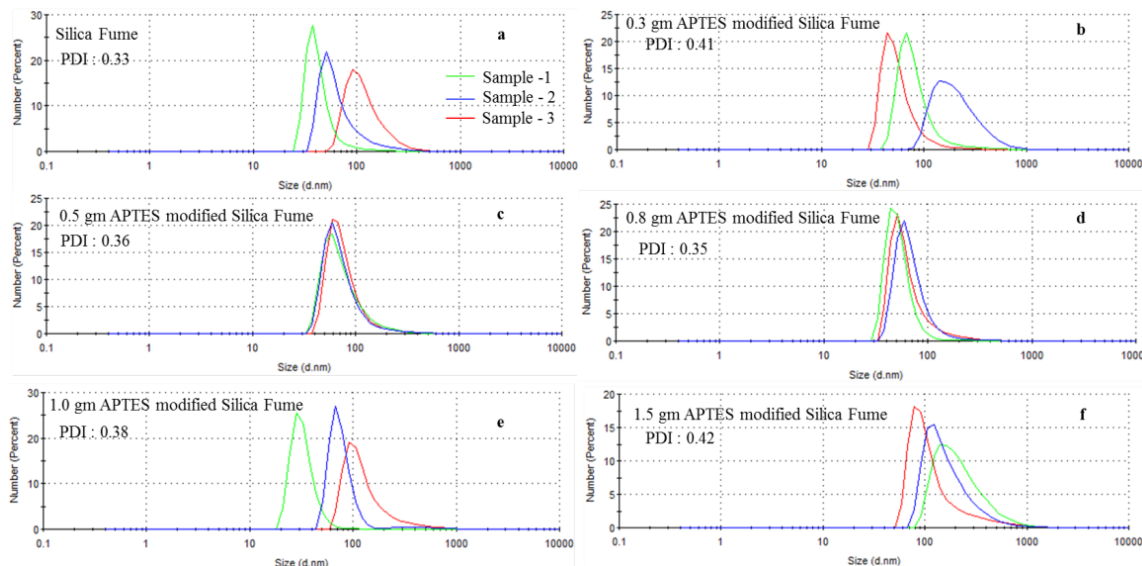


Figure 5. DLS number mean size distribution curves for increasing amount of APTES concentration: (a) pristine silica fume, (b) 0.3 gm APTES, (c) 0.5 gm APTES, (d) 0.8 gm APTES, (e) 1.0 gm APTES, and (f) 1.5 gm APTES.

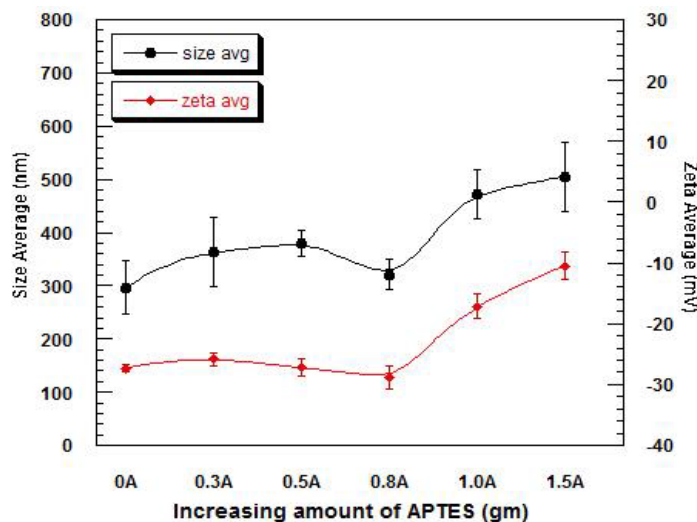


Figure 6. Effect of APTES (amines) functionality on hydrodynamic size and zeta potential (surface charge) of silica fume.

Viscosity Characterization

The viscosity for unaged, (RTFO-aged) and (PAV-aged) binders for the control asphalt (PG 64-22), 8% SFMB, APTES-modified SFMB, and THPMP-modified SFMB were conducted at 20 rpm and 135 °C. **Table 1** shows the average viscosity values. The general trend for all cases is as expected: the unaged and RTFO-aged samples of both APTES- and THPMP-modified SFMB have higher viscosities. For unaged samples, both APTES- and THPMP-modified samples show an increase in viscosity of approximately 10% compared to unmodified SFMB. For RTFO-aged samples, the APTES- and THPMP-modified samples showed an 8% increase in viscosity compared to SFMB samples. For both short- and long-term aged samples, APTES- and THPMP-modified samples show a slight increase in viscosity values compared to control and SFMB, and a large increase compared to Control.

Table 1. Rotational viscosity values.

Aging Level	Control PG 64-22	8% SF	APTES Modified SFMB	THPMP Modified SFMB	APTES+THPMP Modified SFMB
Un-aged	462.5	654	724.8	750	587.5
RTFO	658.3	823	887.5	887.5	987
PAV	1888	2500	2663	2675	2313

The viscosity aging index (VAI) is then calculated to evaluate the extent of aging by using the viscosity results before and after short and long-term aging using eqn (4). The VAI indicates the extent of age hardening in terms of viscosity. The values of the VAI for modified and unmodified specimens at 20 rpm are shown in **Figure 7**.

$$VAI = \frac{\text{Aged viscosity value} - \text{Unaged viscosity value}}{\text{Unaged viscosity value}} \tag{4}$$

As shown in **Figure 7**, the RTFO short-term VAI values for APTES- and THPMP-surface-modified SFMB are overall significantly lower than those of control binder. APTES modification to the 8% SFMB decreased the VAI by 33%. THPMP modification to the 8% SFMB decreased the VAI by 29%. Thus, combining the surface modification of APTES and THPMP to the 8% SFMB reflected the increase in the VAI. However, APTES (containing amine groups) showed a significant decrease in VAI, which is attributed to the reduction in silica fume nanoparticle agglomeration. For PAV long-term aging shown in **Figure 7**, the APTES surface modification to the 8% SFMB decreased the VAI by 5 %, while THPMP functionalization decreased the VAI by 9%. For combination modification, the VAI increased by 4%.

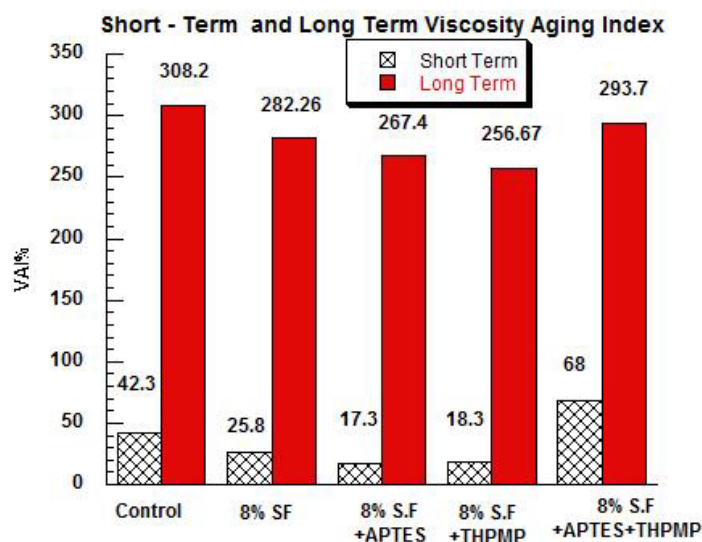


Figure 7. Viscosity aging index for short-term aging and long-term aging. Scanning Electron Microscope (SEM).

As shown in the SEM image of surface-modified 8% SFMB in **Figure 8a**, the microstructure of 8% SFMB was changed when APTES was added to the 8% SFMB. In **Figure 8a** SEM image (APTES-modified silica fume) and in **Figure 2a** (unmodified silica fume), white particles in the image represent the silica fume particles. APTES-modified SF shows better dispersion than the unmodified silica fume asphalt, as there are larger patches particles in unmodified SF than in the APTES-modified SF. This indicates better dispersion of the particles in the APTES-modified SF, while having amine molecules on the SF particles' surface. No dispersion occurred with THPMP to the 8% silica fume modified binder as shown in **Figure 8b**. SEM images of the combination of APTES+THPMP showed better dispersion in asphalt **Figure 8c**.

Complex Modulus (G*) Behavior

The dynamic shear rheometer was used to determine the complex modulus of the samples from 76 °C to 4 °C. From this data, the principle of time-temperature superposition (TTS) was used to determine the factors used to generate the master curves

shown in **Figure 9**. For this DSR results, only the APTES samples were shown. The stiffening effect of the APTES on unaged SF, which was also observed in the RV results, is clearly shown for all reduced frequencies. After aging, the 8% SF has a slightly lower modulus value than the APTES-modified sample; however, after 0.1 rad/s, the two samples show nearly the same moduli values.

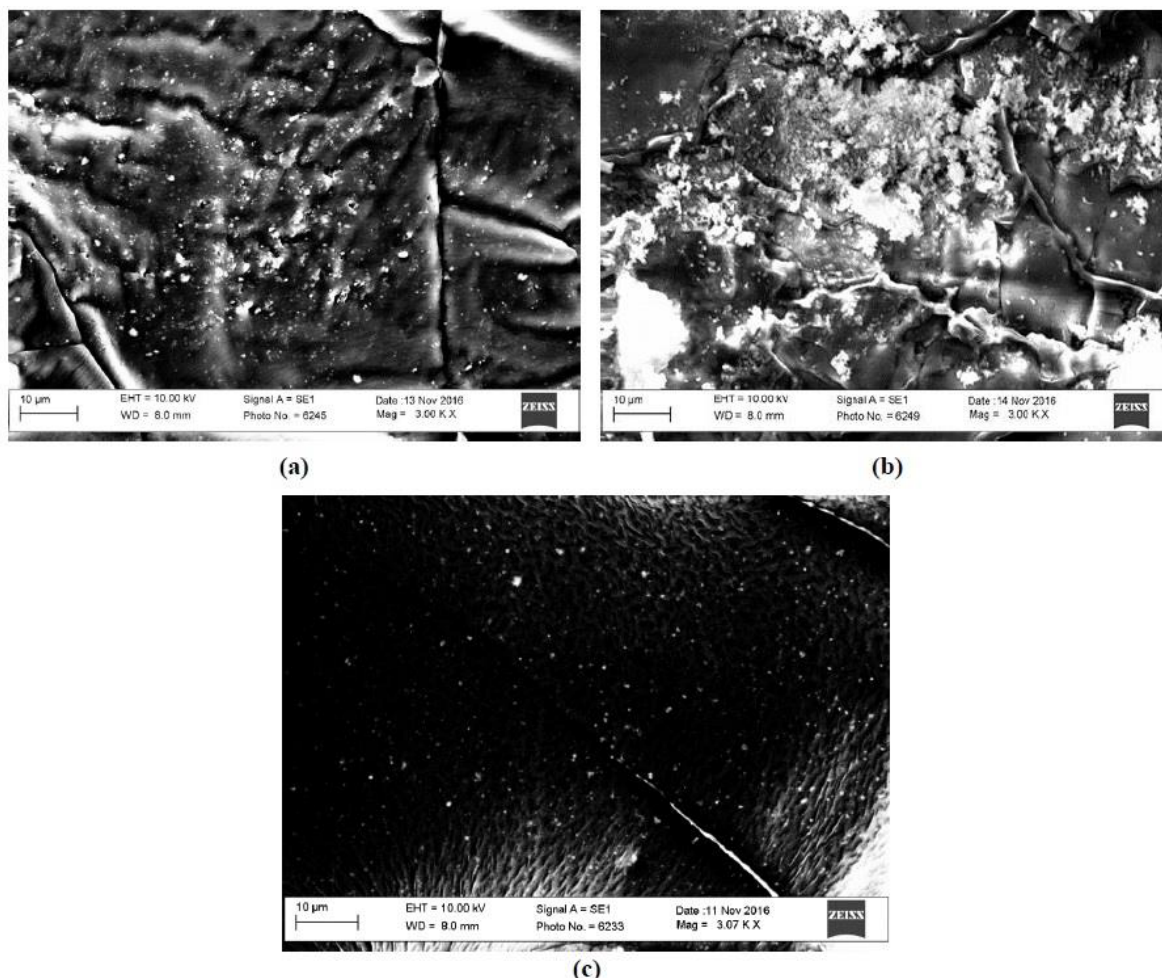


Figure 8. (a) SEM image of APTES-modified 8% silica-fume-modified binder; (b) SEM image of THPMP-modified 8% silica-fume-modified binder; (c) SEM image of combined APTES and THPMP-modified 8% silica-fume-modified binder.

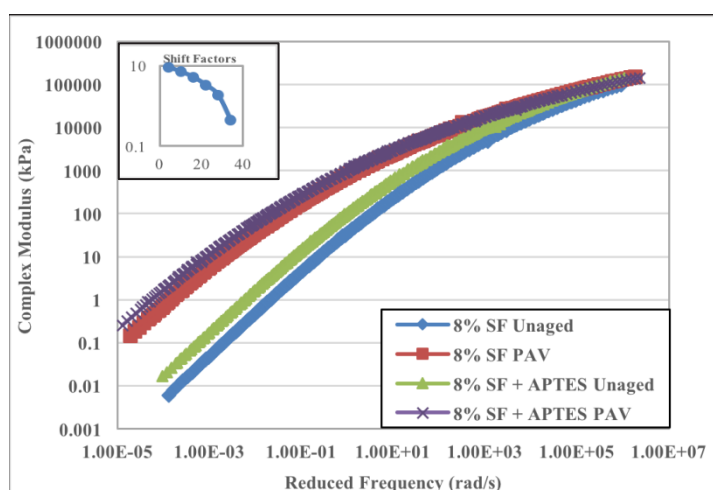


Figure 9. Complex Modulus (G^*) Master Curves for Unaged and PAV SF and for Unaged and PAV SF + APTES from 76 °C to 4 °C.

To further understand the results, the elastic and viscous moduli values were plotted against each other; the point at which the two values are equal was denoted as the crossover frequency, which can be considered as a hardness parameter of the material. Using TTS, the frequencies were converted into temperature values and are shown in **Table 2**. The hardening effect of APTES is clearly shown: the unaged SF+APTES and PAV SF+APTES samples had higher crossover temperatures than the unaged SF and PAV SF samples, respectively [17]. However, when observing the effects of aging on crossover temperature, Δ Crossover Temperature was lower for the APTES samples.

Table 2. Crossover temperatures for 8% SF and 8% SF+APTES.

	Crossover Temperature (°C)	Δ Crossover Temperature (°C)
8% SF Unaged	9.16	18.34
8% SF PAV	27.50	
8% SF+APTES Unaged	13.28	15.13
8% SF+APTES PAV	28.41	

Fourier Transform Infrared Spectroscopy (FTIR)

In **Figure 10**, the spectra for 8% SF and 8% SF+APTES are given. They show very little difference except for the region from 3000 to 2800 cm⁻¹, in which the absorbance for APTES is slightly higher than that of unmodified SF. In **Figures 11 and 12**, the spectra for unaged and PAV aged samples of SF with and without APTES are shown. From both figures, the changes in chemical composition due to oxidative aging are clearly shown.

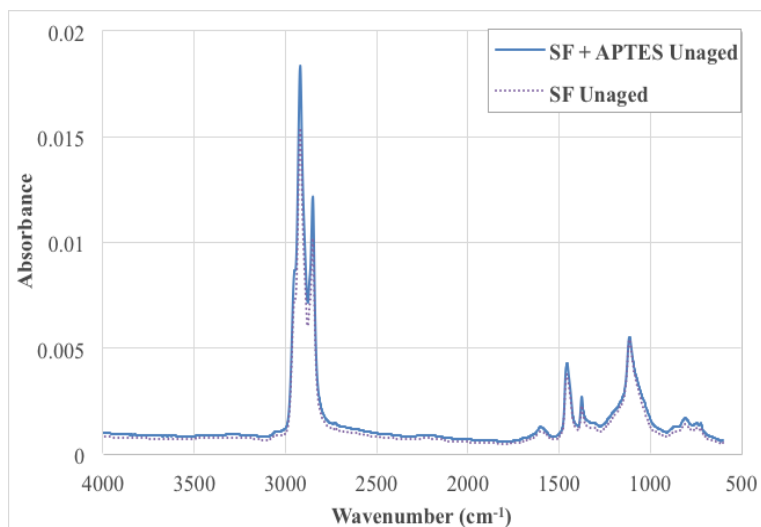


Figure 10. FTIR spectra for 8% SF and 8% SF + APTES from 4000 to 600 cm⁻¹.

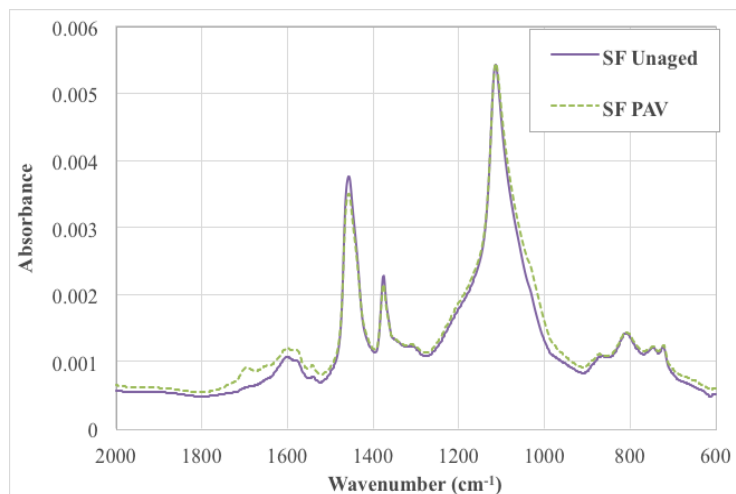


Figure 11. FTIR spectra for 8% SF Unaged and 8% SF PAV from 2000 to 600 cm⁻¹.

After the inclusion of APTES, the changes in the carbonyl and sulfoxide functional group areas due to aging are shown in **Figure 13**, and the Chemical Aging Index (CAI) values are shown in **Figure 13** which were calculated using eqn (5).

$$CAI = \frac{PAV \text{ Aged Peak Area} - \text{Unaged Peak Area}}{\text{Unaged Peak Area}} \tag{5}$$

After the inclusion of APTES, the CAI in the sulfoxide area decreased from 736% to 537%; however, in the CAI in the carbonyl area increased from 123% to 254% (**Figure 13**). Although the inclusion of APTES in SFMB appears to create an increased susceptibility to the formation of carbonyl with aging, the significant reduction in sulfoxide appears to result in improved rheological performance and hence an overall reduction in aging susceptibility.

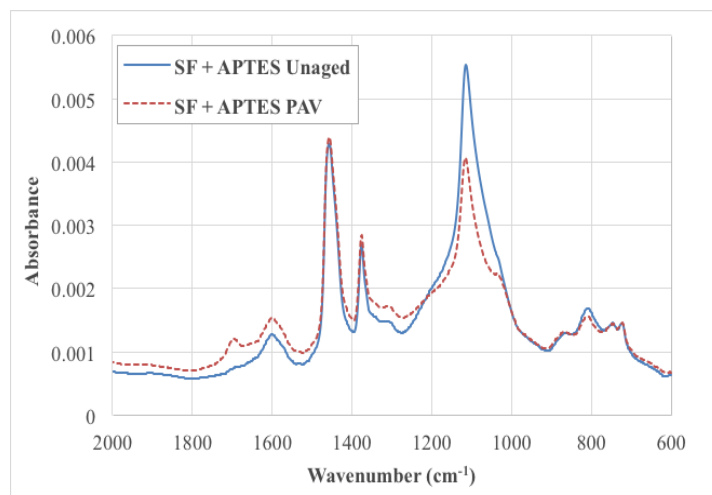


Figure 12. FTIR spectra for 8% SF+APTES Unaged and 8% SF+APTES PAV from 2000 to 600 cm⁻¹

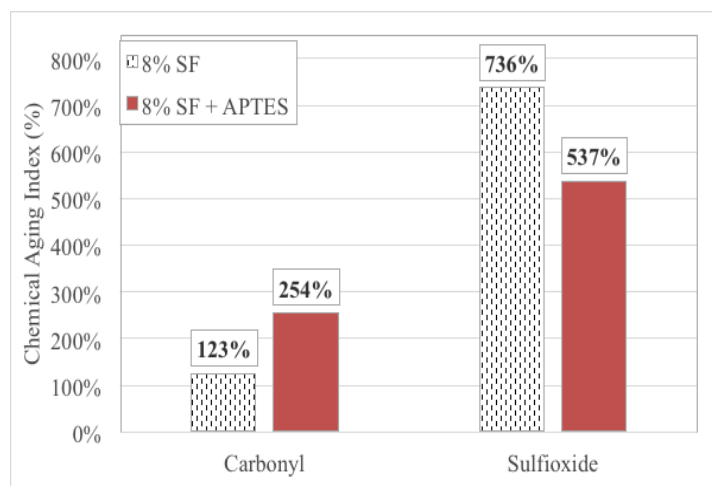


Figure 13. Chemical Aging Index of SFMB without and with APTES.

CONCLUSIONS

The purpose of this study was to evaluate the rheological characteristics of SFMB after surface-modification schemes for the silica fume particles. Based on the test results for APTES- and THPMP-modified SFMB, the following conclusions can be drawn:

1. APTES-modified silica fume particles have better zeta potential than the pristine silica fume particles, which illustrates that amine groups on the surface of the silica fume particles are a good candidate for reducing aging susceptibility of asphalt binder.

2. The viscosity results proved that the APTES-modified SFMB can increase the viscosity of 8% SFMB.

3. Based on the viscosity aging index calculations, APTES (containing amine groups) showed a large decrease in VAI, which is attributed to the reduction in silica fume nanoparticle agglomeration. The better stability of the particle is an indication of lower VAI, which was achieved in APTES+THPMP modified silica fume.

4. SEM images show significant dispersion of APTES-modified SF, which indicates better dispersion than in unmodified silica fumes asphalt. There are larger patches of agglomeration in unmodified silica fume particles than in APTES-modified, which indicates better dispersion of the silica fume particles that have amine molecules on their surface. APTES+THPMP has better dispersion in asphalt, but based on performance APTES showed better results.

5. In terms of complex modulus, the master curves from the dynamic shear rheometer show that APTES slightly increased the 8% SF for both Unaged and PAV aged specimens particularly at low reduced frequency values.

6. APTES modified SF was shown to change the Δ crossover temperature approximately 3 degrees indicating a lower susceptibility to aging.

7. Based on the chemical aging index calculations, the inclusion of APTES in SFMB led to an increase in the formation of carbonyl and a decrease in the formation of sulfoxide. The significant reduction in sulfoxide appears to result in improved rheological performance and hence an overall reduction in aging susceptibility.

ACKNOWLEDGMENTS

This research is sponsored by the University Transportation Center: Center for Highway Pavement Preservation. The contents of this paper reflect the view of the authors, who are responsible for the facts and the accuracy of the data presented. This paper does not constitute a standard, specification, or regulation.

REFERENCES

1. Abutalib N, et al. Investigating Effects of application of Silica Fume to Reduce Asphalt Oxidative Aging. *Am J Eng Appl Sci* 2015;8:176-184.
2. Tarrer AR and Vinay Wagh. The Effect of the Physical and Chemical Characteristics of the Aggregate on Bonding, Auburn University. Auburn, Alabama Strategic Highway Research Program National Research Council Washington, D.C., USA 1991.
3. Miller JC, Vicenzi SJ. Phosphate ester asphalt additives. US 5820663 A, 1998.
4. Bagwe RP, et al. Surface Modification of Silica Nanoparticles to Reduce Aggregation and Nonspecific Binding. *Langmuir* 2006;22:4357-4362.
5. Hui Yao and Zhanping You. Effectiveness of Micro and Nanomaterials in Asphalt Mixtures through Dynamic Modulus and Rutting Tests. *J Nanomater Appl Sci* 2016;16.
6. Alejandra B, et al. Influence of nanosilica and diatomite on the physicochemical and mechanical properties of binder at unaged and oxidized conditions. *Constr Build Mater J* 2016;127:176-182.
7. Maciej G, et al. De-agglomeration and homogenisation of nanoparticles in coal tar pitch-based carbon materials. *J Springer Appl Sci* 2016;18-56.
8. Guangji Xu and Hao Wang. Molecular dynamics study of oxidative aging effect on asphalt binder properties. *Fuel J* 2017;188:1-10.
9. ASTM. D2872 Standard Test Method for Effect of Heat and Air on a Moving Film of Asphalt (Rolling Thin-Film Oven Test) ASTM: American Standard Testing Methods, 2004.
10. ASTM. D6521 Standard practice for accelerated aging of asphalt binder using a pressurized aging vessel (PAV) ASTM: American Standard Testing Methods, 2010.
11. ASTM. D4402 Standard Test Method for Viscosity Determination of Asphalt at Elevated temperatures Using a Rotational Viscometer. ASTM: American Standard Testing Methods, 2006.
12. ASTM. D7175 Standard Test Method for Determining the Rheological Properties of Asphalt Binder Using a (Dynamic Shear Rheometer) ASTM International, 2015.
13. ASTM International. Products and Services, Standards and Publications 2013.
14. Fini EH. Preparation and uses of bio-adhesives. US Patent App., 2013;14/032,445.
15. Fini, et al. Chemical characterization of biobinder from swine manure: Sustainable modifier for asphalt binder. *J Mater Civil Eng* 2011;23:1506-1513.
16. Fini, et al. Partial replacement of asphalt binder with bio-binder: characterisation and modification. *Int J Pavement Eng* 2012;13:515-522.
17. Gapinski G and Scanlon J. Silica Fume. Norchem, Inc. 2011.